Frost matters: Incorporating late-spring frost in a dynamic vegetation model regulates regional productivity dynamics in European beech forests

Benjamin F. Meyer[1], Allan Buras[1], Konstantin Gregor[1], Lucia S. Layritz[1], Adriana Principe[2], Jürgen Kreyling[3], Anja Rammig[1], and Christian S. Zang[4]

[1]Technical University of Munich, Professorship of Land Surface-Atmosphere Interactions, TUM School of Life Sciences, Freising, Germany
[2]cE3c - Centre for Ecology, Evolution and Environmental Changes (cE3c-FCUL), Faculdade de Ciências da Universidade de Lisboa, Campo Grande, Lisboa, Portugal
[3]Institute of Botany and Landscape Ecology, University of Greifswald, Partner in the Greifswald Mire Centre, Greifswald, Germany
[4]Institute for Ecology and Landscape, Weihenstephan-Triesdorf University of Applied Sciences, Freising, Germany

Correspondence: Benjamin F. Meyer (ben.meyer@tum.de)

Abstract. Late-spring frost (LSF) is a critical factor influencing the functioning of temperate forest ecosystems. Frost damage in the form of canopy defoliation impedes the ability of trees to effectively photosynthesize, thereby reducing tree productivity. In recent decades, LSF frequency has increased across Europe, likely intensified by the effects of climate change. With increasing warming, many deciduous tree species have shifted towards earlier budburst and leaf development. The earlier start of the growing season not only facilitates forest productivity but also lengthens the period during which trees are most susceptible to LSF. Moreover, recent forest transformation efforts in Europe intended to increase forest resilience to climate change have focused on increasing the share of deciduous species in forests. To assess the ability of forests to remain productive under climate change, dynamic vegetation models (DVMs) have proven to be useful tools. Currently, however, most state-of-the-art DVMs do not model processes related to LSF and the associated impacts. Here, we present a novel LSF module for integration with the dynamic vegetation model LPJ-GUESS. This new model implementation, termed LPJ-GUESS-FROST, provides the ability to directly attribute impacts on simulated forest productivity dynamics to LSF. We use the example of European beech, one of the dominant deciduous species in Central Europe, to demonstrate the functioning of our novel LSF module. Using a network of tree-ring observations from past frost events we show that LPJ-GUESS-FROST can reproduce productivity reductions caused by LSF. Further, to exemplify the effects of including LSF dynamics in DVMs, we run LPJ-GUESS-FROST for a study region in southern Germany for which high-resolution climate observations are available. Here, we show that modeling LSF plays a substantial role in regulating regional NPP and biomass dynamics emphasizing the need for LSF to be more widely accounted for in DVMs.

1 Introduction

20 In temperate climates, late-spring frost (LSF) plays a critical role in the functioning of forest ecosystems (Grossman, 2023). Below-freezing temperatures during the early stages of leaf development damage photosynthetic tissue (Inouye, 2000; Chen et al., 2023), hamper secondary growth (Dittmar et al., 2006; Príncipe et al., 2017), induce mobilization of stored C reserves to repair damaged tissues (D'Andrea et al., 2019), and ultimately constrain the range limits of affected tree species (Körner et al., 2016; Kollas et al., 2014a). Consequently, evidence suggests that ~~late-spring frost~~

25 LSF substantially reduces forest ecosystem productivity (Hufkens et al., 2012).

The frequency of LSF has increased across Europe in recent decades displaying a trend that will likely be exacerbated under a changing climate~~(Zohner et al., 2020)~~, as an earlier start of the growing season leads to the timing of leaf-out and periods with high likelihood for frost to increasingly coincide (Zohner et al., 2020; Ma et al., 2019). Due to increasing warming, many deciduous tree species have experienced a shift towards earlier budburst, flowering, and

30 subsequent leaf development (Morin et al., 2009; Menzel et al., 2001). While a longer growing season facilitates forest productivity (Keenan et al., 2014; Duveneck and Thompson, 2017), it may also bear a greater risk of detrimental LSF impacts as the period in which trees are most susceptible increases (Ma et al., 2019; Sangüesa-Barreda et al., 2021, Chamberlain and Wolkovich (2021)). Thus, it is unclear to what extent climate change will alter the impact of LSF on forest ecosystem productivity.

35 One of the main tree species in central Europe is *Fagus sylvatica* (European beech), which under potential natural vegetation is the dominant species across large regions of the European landscape (Bohn and Welß, 2003). Although historic land management has reduced the proportion of European beech in forests, recent management efforts have focused on re-establishing a higher share of deciduous broadleaf species, including beech (Kenk and Guehne, 2001; Schütz, 1999). These efforts aim to increase forest resilience to climate change (Yousefpour et al., 2018). In a simple

40 twist of fate, European beech tends to be relatively susceptible to late-spring frost which consequently co-determines its range limits across Europe (Gazol et al., 2019; Menzel et al., 2015; Kollas et al., 2014a; Bolte et al., 2009). Since beech has also been shown to be negatively impacted by drought events (Meyer et al., 2020; Dulamsuren et al., 2017; Zimmermann et al., 2015; Scharnweber et al., 2011), the success of recent forest transformation efforts hinges on the ability of beech forests to remain productive in its current distribution range under climate change.

45 In this context, dynamic vegetation models (DVMs) are a useful tool to assess the impact of climate change and extreme events on forest productivity (Yao et al., 2022; Medlyn et al., 2011; Gampe et al., 2021; Rammig et al., 2010). Nevertheless, most current, state-of-the-art DVMs do not simulate LSF and the associated consequences, possibly overestimating the positive effects of climate change (e.g., longer growing seasons) on the carbon sequestration potential of temperate forest ecosystems (Liu et al., 2018), and underestimating detrimental effects from climate

50 change related impacts on tree health and mortality. Considering forests currently account for nearly 50 percent of terrestrial net primary productivity (NPP) (Bonan, 2008), the ability to assess the impact of current and future

LSF on forest NPP via vegetation modeling is crucial. To breach this gap, we present a novel late-frost module for integration with the dynamic vegetation model LPJ-GUESS (Smith et al., 2014; Hickler et al., 2012). A phenological model to predict ~~leaf-out~~ bud-burst, introduced by Kramer et al. (2017), forms the basis of this new model and allows us to intersect the start of leaf-development with the occurrence of sub-zero temperatures. The integration with LPJ-GUESS – named LPJ-GUESS-FROST – enables us to model productivity dynamics and directly attribute them to the presence (or absence) of LSF.

The new model implementation is validated against a regional tree-ring network and, subsequently, we present the effect of LSF on European beech NPP and carbon stocks, determine shifts in intra-tree C allocation patterns as predicted by the model, and identify regional LSF hotspots across our study region.

2 Methods

In 1953 and 2011, well-documented late-frost events occurred across large regions of Bavaria. The 1953 event was centered around the alps and alpine foothills in southern Bavaria, the 2011 event had its epicenter in Franconia in northern Bavaria. In both cases, freezing damage was observed in European beech ~~. Here, we develop a novel frost module for the DVM LPJ-GUESS, validate it against observations from the two LSF events , ~~ (Príncipe et al., 2017; Dittmar et al., 2006). We make use of these two observed events to validate our frost implementation in LPJ-GUESS-FROST and analyze the impact of LSF on European beech productivity and biomass across Bavaria.

2.1 Overview of the dynamic vegetation model LPJ-GUESS

We use LPJ-GUESS (Version 4.0.1, Lindeskog et al. (2017)), a well established dynamic vegetation model designed to simulate ecosystem processes on regional to global scale (Smith et al., 2001, 2014). Vegetation is represented by plant functional types (PFTs) which cycle through establishment, growth, competition, and mortality. Generally, a PFT groups attributes (phenology, life-strategy, drought-tolerance, bioclimatic limits, etc.) of multiple, similar individual species and represents them through a set of parameters. In this study, we follow the commonly used parameterization of Hickler et al. (2012), developed specifically for European tree species, to explicitly simulate European beech. The model is driven by gridded daily climate, soil texture, nitrogen deposition, and global atmospheric CO_2 (for a more detailed description see section "Modeling protocol"). Processes are modeled on a gridcell basis where the spatial resolution of the gridcells follows the spatial resolution of the climate inputs.

The processes modeled by LPJ-GUESS to simulate primary production and growth include photosynthesis and stomatal conductance based on BIOME3 (Sykes and Prentice, 1996), allocation of NPP to various compartments based on allometric constraints (Sitch et al., 2003), stochastically simulated population dynamics (Hickler et al., 2004)

and biomass-destroying disturbance, and nitrogen, soil and litter processes (Smith et al., 2014). Simulated vegetation dynamics emerge from the interaction of growth and competition for resources (e.g. light, water, nutrients). For each gridcell multiple replicate patches are simulated, each of which represents a random sample of the gridcell, to account for idiosyncracies in disturbance and stand development of different vegetation stands. Within each patch, a single average individual represents cohorts of individuals established in a given year with all individuals of a given cohort sharing the same size and form as they grow.

A key process in the context of this study is summergreen leaf phenology which is explicitly modeled in LPJ-GUESS as a function of daily mean temperature following a generalized chilling and growing-degree day model (Smith et al., 2001). Chill days occur when daily mean temperature falls below 5°C and, combined with PFT specific parameters regulating the thermal requirement for budburst (GDD_{base}, Equation 1), determine the length of dormancy.

$$GDD_{base} = k_{chill,a} + k_{chill,b} * e^{k_{chill,k} * \text{chilldays}} \tag{1}$$

Subsequently, when a sufficient growing degree ~~days (days with temperature >~~ sum (GDD_5, Equation 1, mean temperature (T) over 5°C),

$$GDD_5 = max\{0, T-5\} \tag{}$$

for a given PFT ~~have~~ has accumulated, leaf unfolding commences and the phenological status (phen, Equation 2) is updated daily as a fraction of complete canopy cover, ranging between 0 and 1, until maximum canopy cover is reached:

$$\text{phen} = \begin{cases} 0, & GDD_5 \leq GDD_{base} \\ \min\{1, \frac{GDD_5 - GDD_{base}}{GDD_{ramp}}\}, & GDD_5 > GDD_{base} \end{cases} \tag{2}$$

where GDD_{ramp} is a PFT parameter.

2.2 Implementation of bud-burst model and late-spring frost in LPJ-GUESS

We ~~extend~~ extended the leaf phenology calculation in LPJ-GUESS by implementing a novel model simulating LSF, running in parallel to the standard LPJ-GUESS phenology module (see Figure A2). Late-spring frost is primarily a disruption of the phenological cycle of leaf development caused by the overlap of leaf-out and a sub-zero, critical leaf temperature. The standard implementation of LPJ-GUESS phenology merely calculates the fraction of complete

canopy cover (see above), thus, we here ~~use~~ used a more specific model for calculating ~~leaf-out~~ bud-burst status from Kramer et al. (2017). This sequential, two-stage chilling and forcing model relies on daily mean temperature to calculate the ~~leaf-out~~ bud-burst status, returning 0 when ~~leaf-out~~ bud-burst has not yet occured and 1 when ~~leaf-out~~ bud-burst has taken place. The first stage of the model is the chill state (S_c, Equation 3) which determines the period of phenological rest, calculated as

$$S_c(t) = \sum_{i=t_0}^{t} R_c(T_i) \tag{3}$$

where t_0 is November 1st the day on which the phenological model resets, t is the current timestep (i.e. day), T_i is the mean air temperature at timestep i. $R_c(T_i)$ is the the rate of chilling as a function of the mean air temperature at time i formulated as

$$R_c(T) = \begin{cases} 0, & T < T_{c,min} \\ \frac{T - T_{c,min}}{T_{c,opt} - T_{c,min}}, & T_{c,min} \leq T \leq T_{c,opt} \\ \frac{T - T_{c,max}}{T_{c,opt} - T_{c,max}}, & T_{c,opt} \leq T \leq T_{c,max} \\ 0, & T > T_{c,max} \end{cases} \tag{4}$$

where $T_{c,min}$, $T_{c,opt}$, and $T_{c,max}$ are the minimum, optimum, and maximum mean air temperature required to advance chilling.

Analogously, the forcing state (S_f, Equation 5) is calculated as the running sum of the forcing rate (R_f, Equation 6).

$$S_f(t) = \sum_{i=t_1}^{t} R_f(T_i) \tag{5}$$

$$R_f(T) = \begin{cases} 0, & T < T_{f,min} \\ \frac{1}{1 + e^{a_f(T + b_f)}}, & T > T_{f,min} \end{cases} \tag{6}$$

Where t_1 is the time at which the chill state reaches the critical value $S_{c,crit}$, a species-specific constant derived from empirical observations determining the end of the chilling period, $T_{f,min}$ is the minimum mean air temperature required for forcing, and a_f and b_f are species-specific, fitted constants. Subsequently, ~~leaf-out~~ bud-burst occurs

(i.e. model state = 1) when the forcing state (S_f) attains a critical value $S_{f,crit}$, which, like the critical value for chilling ($S_{c,crit}$) is derived from empirical observations.

In a second step we cross-reference the ~~leaf-out~~ bud-burst status (0 or 1) with the daily minimum temperature (T_{min}) to determine late-frost status. When ~~leaf-out~~ bud-burst has already occured (~~leaf-out~~ bud-burst status = 1) and T_{min} crosses a temperature threshold T_{frost} late-frost occurs. Accordingly, we calculate LSF as

$$LSF(leafout, T_{frost}, T_{min}) = \begin{cases} 1, & leafout = 1 \text{ and } T_{min} < T_{frost} \\ 0, & else \end{cases}$$

$$LSF(leafout, T_{frost}, T_{min}) = \begin{cases} 1, & leafout = 1 \text{ and } T_{min} < T_{frost} \\ 0, & else \end{cases} \tag{7}$$

To approximate the generally localized effect of LSF we model T_{frost} stochastically for each individual patch by randomly drawing from a gaussian distribution with mean T_{frost_μ} and standard deviation T_{frost_σ} (for details, see Section 2.7 and Figure A1). A full list of the parameter values for Equations 1 - 5 is shown in Section 2.7 (Table 1).

Late-frost damage is modeled as the phenology status (where 0 indicates no canopy and 1 indicates full canopy) being reset to zero (i.e. complete removal of existing leaves), followed by a leafless period ~~(Menzel et al., 2015; Rubio-Cuadrado et al., 2021; Nolè et al., 2018)~~ after which the phenological state continues to advance until it reaches full canopy coverage. We implemented a constant leafless period based on observations from several studies (Menzel et al., 2015; Rubio-Cuadrado et al., 2021; Nolè et al., 2018) which found that the time between frost and full development of the second cohort of leaves ranged between ~ 40 and ~ 80 days. Consequently, we implement a 40-day leafless period where trees have no leaves, followed by a 20-day re-greening period where phenology steadily increases to 1 (i.e. full leaf coverage).

Since we model late-frost damage stochastically (as a function of T_{frost_μ} and T_{frost_σ}) for each patch, this means that any given gridcell will have late-frost damage ranging between 0% and 100%. For example, if none of the patches experience frost the gridcell has 0% frost damage. If half of the patches experience frost, the gridcell has 50% frost damage. Through this mechanism we approximate a continuous function for frost damage.

The additional carbon necessary to rebuild the canopy after LSF is drawn from the carbon storage pool in LPJ-GUESS-FROST. Carbon allocation in LPJ-GUESS occurs at the end of the year by distributing the accumulated NPP to the various biomass compartments according to a set of allometric constraints. If the accumulated NPP is not sufficient to allocate enough carbon to each compartment to satisfy these constraints,

additional carbon can be "borrowed" from a carbon storage pool. This pool must be re-filled when enough NPP is available. The carbon lost due to LSF is calculated as the total carbon allocated to leaves for a given year multiplied by the fraction of canopy coverage at the time of LSF. At the end of the year, during allocation, this fraction of carbon is deducted from the storage pool. A portion of this is immediately "repaid", reducing the amount of carbon available for allocation to the structural compartments. Over subsequent years, more NPP is allocated to the storage pool until it is completely refilled.

2.3 Site-level tree-ring data

To validate the results of LPJ-GUESS-FROST we ~~utilize~~ utilized a tree-ring network consisting of previously published data from 21 sites that were affected by LSF events in 1953 (Dittmar et al., 2006) and 2011 (Príncipe et al., 2017) supplemented by data from 5 sites from the epicenter of the 2011 LSF that have been newly sampled for this study. These data ~~allow~~ allowed us to retrospectively analyze the effect of LSF on productivity in European beech. Radial growth – expressed as ring-width – integrates multiple signals aside from age and climate and can be used as an indicator of variation in forest productivity (Xu et al., 2017). In the aggregate, the ring-width of a given year is composed of age-/size-, climate-, and disturbance-related trends and additional, often unexplained variability (Cook, 1987). Nonetheless, ring-width data have proven a useful tool to investigate the effect of climate on tree growth ~~(e.g. Jevšenak, 2019; Anderegg et al., 2020; Zang et al., 2014; Bhuyan et al., 2017; Wilmking et al., 2020)~~ (e.g., Jevšenak, 2019; Anderegg et al., 2020; Zang et al., 2014; Bhuyan et al., 2017; Wilmking et al., 2020). To isolate the climate signal all tree-ring width data were detrended with a cubic spline with a frequency cutoff of 0.5 at 30 years. Detrending removes age-related growth trends from tree-ring data. The residuals of the determined spline, also called ring-width indices (RWI), consequently depict mainly climate-induced growth variations (Sullivan et al., 2016; Cook and Peters, 1997). Following detrending, the individual tree-ring series (ranging from 10 to 30 per site) were aggregated to site-level chronologies. The median, minimum, and maximum length of raw tree-ring chronologies is 113 years, 32 years, and 227 years, respectively. Since the climate data used to drive LPJ-GUESS-(FROST) begins in 1951, any RWI before that year were not included in subsequent analyses. Consequently, the median, minimum, and maximum length of the detrended ring-width chronologies used for comparison with LPJ-GUESS-(FROST) is 62 years, 33 years and 68 years, respectively. The median, minimum, and maximum sample size for the site-level chronologies is 20, 10, and 30 individual tree-ring series, respectively (Figure A3).

2.4 Forest condition monitor data

To complement the validation of LPJ-GUESS-FROST via tree-rings, we conducted an analysis of the 2011 LSF using remote sensing data from the European Forest Condition Monitor (EFCM, Buras et al. (2021)). The EFCM provides high-resolution, relative measures of forest greenness based on the Terra Moderate Image Resolution Imaging

Normalized Difference Vegetation Index (MODIS, NDVI) (Buras et al., 2021). The key value used in the context of this study is the EFCM's proportional deviation from the median (PDM) metric. This metric facilitates the comparison of absolute changes in NDVI between pixels, i.e., pixels with a lower PDM can be said to display less relative greenness than pixels with a high PDM as referenced against the long-term median (Buras et al., 2021). To quantify the impact of the LSF on May 4th, 2011 we used the PDMs from May 25th. Since the EFCM provides data integrated at a 16-day interval, this ensured that the entire post-LSF response was depicted in the PDMs. PDMs from an earlier timestep would have necessarily also included pre-LSF signals. Additionally, we cross-referenced the PDMs with the regions of Bavaria that experienced sufficiently negative temperatures for LSF (see Table 1) on May 4th.

2.5 Climate data

We use two separate climate datasets to force LPJ-GUESS-(FROST) for this study. To reproduce the known, site-level frost events in 1953 and 2011, we used historic, thin-plate spline interpolated, daily climate station observations (mean temperature, minimum temperature, precipitation) from the German Meteorological Service (DWD) as downloaded from the climate data center (CDC, https://www.dwd.de/DE/klimaumwelt/cdc/cdc_node.html). For each day over the analyzed period (1951-2020), available observations from on average 227 climate stations (range 182-243 stations per day) were mapped to a digital elevation model (SRTM 90, https://cgiarcsi.community/data/srtm-90m-digital-elevation-database-v4-1/) with a spatial resolution of 250 m x 250 m using a 3-dimensional thin-plate spline (function TPS in the 'fields' package) with longitude, latitude, and elevation as predictors for the temperature field. This was done to account for elevational effects on minimum temperatures, which is a particularly important aspect when applying critical temperature thresholds for LSF-mapping. Grid sizes of commonly used gridded products (e.g., 0.1°) render too coarse in regions with a heterogeneous topography to resemble represent small scale variations in minimum temperature. The mean RMSE of mapped vs. observed temperatures was 0.43 ± 0.24 K (mean ± sd).

To analyze the regional variation of LSF dynamics across Bavaria we instead used the BayObs gridded, daily climate data product provided by the Bavarian Environment Agency (LfU). This dataset provides historical, daily mean temperature, daily minimum temperature, and daily precipitation sum from 1951 until 2020 on a 5km spatial resolution for the Bavarian domain (Bayerisches Landesamt für Umwelt [Hrsg.], 2020). We used this dataset to avoid the excessive computational load associated with running Bavaria-wide simulations at a resolution of 250 m by 250 m.

2.6 Modeling protocol

We conducted two separate simulation experiments. Firstly, to determine the ability of LPJ-GUESS-FROST to reproduce the effect of known LSF on European beech growth we forced LPJ-GUESS and LPJ-GUESS-FROST with

the historic, spline-interpolated climate data for the 26 sites of our tree-ring network. Secondly, to ascertain the wider impact and regional variation of LSF on European beech productivity and biomass dynamics we forced LPJ-GUESS and LPJ-GUESS-FROST with the BayObs data for the entire Bavarian domain. Aside from the climate inputs, we used the same modeling ~~protocoll~~ protocol for both sets of simulation experiments.

To ensure that the simulated ecosystems were in near-equilibrium at the start of the simulation experiment period, we spun up the model for 1000 years using recycled climate data from the first 30 years of the climate inputs. To establish a reference baseline we used LPJ-GUESS for the spinup, that is the version of the model *without* LSF. During the spinup, stochastic disturbances were turned on to facilitate a heterogeneous age-structure of the simulated forests. Subsequently, we used the identical post-spinup state to start the simulation experiment period (1951-2020) runs for both LPJ-GUESS and LPJ-GUESS-FROST. To isolate the effect of LSF on productivity and biomass dynamics we switched off stochastic disturbances in the simulation experiment period. This ensured that any diverging responses in productivity were introduced only in the simulation period and allowed us to more accurately attribute the effect of LSF on these responses.

2.7 Model parameterization

We adapted the commonly used parameterization of LPJ-GUESS for European tree species of Hickler et al. (2012), to simulate ~~European beech~~monospecific European beech stands. The central parameters for the new frost module are described in Table 1. We used 25 replicate patches and, when applicable (i.e. during spinup) a disturbance interval of 200 years.

The frost threshold, i.e. the temperature at which leaves of European beech are damaged, is a source of some uncertainty (Chen et al. (2023)) . Commonly, a threshold of -2.2°C is used for the False Spring Index (Schwartz, 1993; Schwartz et al., 2006; Ma et al., 2019) and remote-sensing observations have indicated significant differences in canopy greenness between ~~frost affected and unaffected~~ frost-affected and -unaffected beech at a minimum temperature of -1°C (Buras et al., 2021). Here, we conducted a sensitivity analysis to determine the frost threshold (-1.65°C $\pm$ 0.85°C) by varying the frost threshold and assessing at which point the simulated response no longer matched the observed RWI response (see ~~A1~~ Figure A1 for details). Our threshold falls well within the mid-range of temperatures at which significant correlations of late-spring frost severity and GPP were found by Chen et al. (2023).

2.8 Model evaluation

To assess the efficacy of LPJ-GUESS-FROST at simulating LSF we cross-referenced simulated NPP with the observed RWI. For both metrics (NPP and RWI), we computed the resistance index (R_t) introduced by Lloret et al. (2011). This index quantifies the ratio of radial growth in an event year (e.g.~~,~~ a frost year) to pre-disturbance growth. In this context, growth during and before a disturbance are defined as the average growth performance across a fixed time

Table 1. Parameter values used ~~in~~ for ~~leaf-out (b)~~ bud-burst and LSF ~~(a)~~ determination in LPJ-GUESS-FROST. Values for ~~leaf-out~~ bud-burst calculation (b) follow those published in Kramer et al. 2017. The parameter values for the frost threshold (a) were determined using a sensitivity analysis comparing LPJ-GUESS-FROST output with RWI data from our study sites (see SI for detail).

T_{frost_μ}[a]	T_{frost_σ}[a]	$T_{c,min}$[b]	$T_{c,opt}$[b]	$T_{c,max}$[b]	a_f[b]	b_f[b]	$S_{c,crit}$[b]	$S_{f,crit}$[b]
-1.65°C	0.85°C	-19.61°C	-0.24°C	77.13°C	-0.1	-32.58	125.51	3.58

period (Lloret et al., 2011). The direct impacts of LSF dynamics are ~~contained~~ confined to a single vegetation season,
consequently we only consider growth performance in the frost year to quantify performance during disturbance. We used a two-year pre-disturbance window – in contrast to the more commonly used three-year window (Pretzsch et al., 2013) – since the first LSF occurred in 1953 and our climate data starts in 1951. Hence, R_t in this study solely refers to impact of LSF on growth in comparison to the two years preceding LSF. We assessed statistical differences in the R_t of LPJ-GUESS, LPJ-GUESS-FROST, and RWI to LSF using a pairwise Wilcoxon rank test (Bauer, 1972).

Additionally, to analyze the impact of LSF on European beech productivity across Bavaria we calculated the loss of NPP and biomass due to LSF as the difference between the output of LPJ-GUESS and LPJ-GUESS-FROST during the post-spinup simulation period from 1951 to 2020.

Post-processing of model output, subsequent statistical analysis, and manuscript authoring was done in R version 4.2.1 (R Core Team, 2022) with addition of the following packages: meta-package tidyverse (Wickham et al., 2019) , dplR (Bunn et al., 2022), fields (Douglas Nychka et al., 2021) ggthemes (Arnold, 2021), here (Müller, 2020), janitor (Firke, 2021), multcompView (Graves et al., 2019), ncdf4 (Pierce, 2022), patchwork (Pedersen, 2020), RANN, rnaturalearth (Massicotte and South, 2023), rnaturalearthhires (South et al., 2024), (Arya et al., 2019), terra (Hijmans, 2022), scico (Pedersen and Crameri, 2022), sf (Pebesma, 2018), zoo (Zeileis and Grothendieck, 2005).

3 Results

3.1 Model validation

The negative impact of LSF on RWI is evident in both documented frost years. In 1953, RWI was reduced to nearly 45 percent of the pre-frost period. The impact of the 2011 frost was less severe, reducing RWI to roughly 70 percent of the pre-frost baseline (Figure 1).

LPJ-GUESS simulated a slightly higher NPP in both frost years than in the pre-frost period (indicated by $R_t > 1$ in Figure 1) and in both 1953 and 2011 R_t from LPJ-GUESS was significantly different from RWI R_t. In contrast, LPJ-GUESS-FROST simulated a substantial reduction in NPP ($R_t < 1$) in both years. In 2011, the impact of

the LSF on productivity is of similar magnitude in both the tree-ring data ($\tilde{R}_t = 0.69$) and LPJ-GUESS-FROST (~~$\tilde{R}_t = 0.49$)albeit significantly more pronounced in the simulated data~~$\tilde{R}_t = 0.55$). For the 1953 LSF, the pattern is similar. LPJ-GUESS-FROST simulates a significant NPP reduction (~~$\tilde{R}_t = 0.59$~~$\tilde{R}_t = 0.57$) in response to LSF, and no significant difference is seen between LPJ-GUESS-FROST and the tree-ring data ($\tilde{R}_t = 0.45$).

For the 2011 LSF, the remote sensing analysis confirms the negative impact due to frost. In the areas of Bavaria that experienced temperatures below the frost threshold of -1.65°C on May 4th, the PDMs were substantially lower than in the areas not affected by LSF (Figure A4).
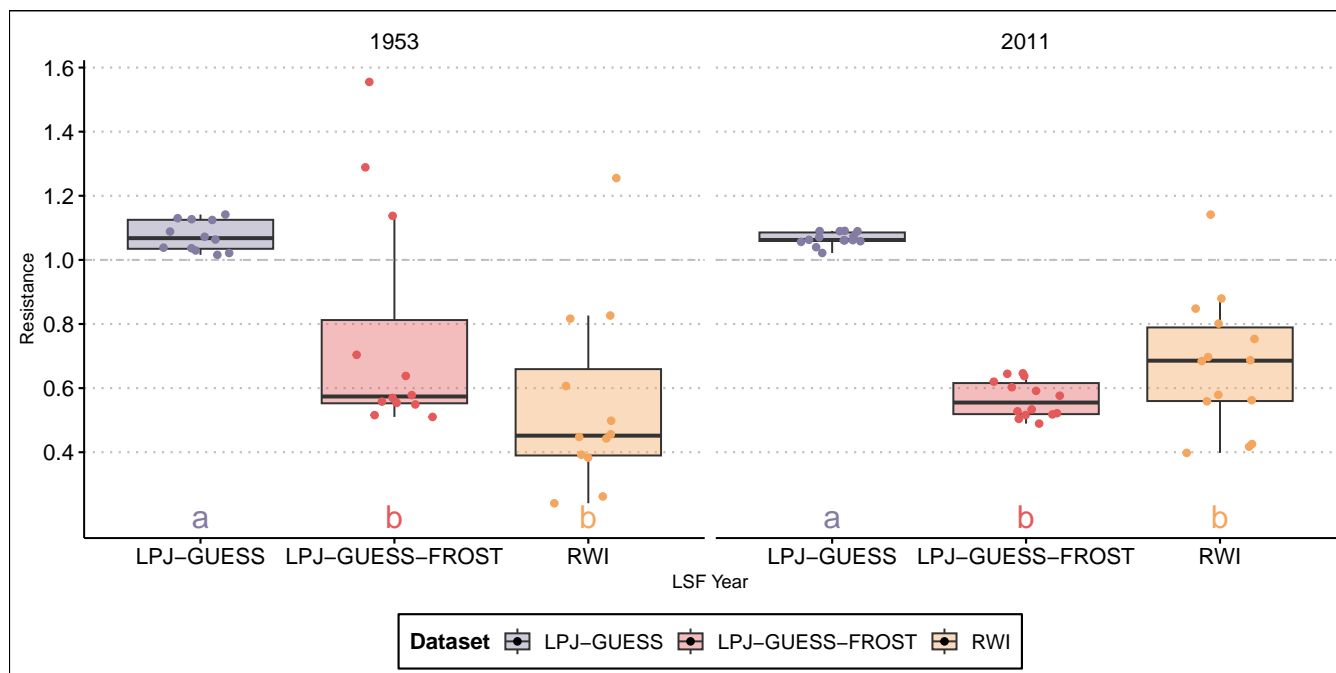
Figure 1. Resistance of observed radial growth and simulated NPP to two well-documented late-frost events. LPJ-GUESS-FROST manages to capture the late-frost signal in both cases, albeit with a larger spread in 1953. The boxplots show the median, quartiles and 1.5 interquartile range. Lettering indicates homogenous groups based on a pairwise Wilcoxon rank sum test with Bonferroni correction for multiple testing.

3.2 Effects on productivity

The range of NPP across all gridcells in Bavaria ~~is quite narrow~~ varied from nearly 0.3 kg C m^{-2} to around 0.6 kg C m^{-2} in LPJ-GUESS. Introducing late-frost dynamics ~~increases~~ increased the variation in NPP ~~across gridcells in any given year~~ to range from ca. 0.15 kg C m^{-2} to 0.6 kg C m^{-2} across all gridcells, as some regions suffer from heavily decreased productivity in response to late-frost damage (Figure 2). Simulated NPP in frost years was roughly 50
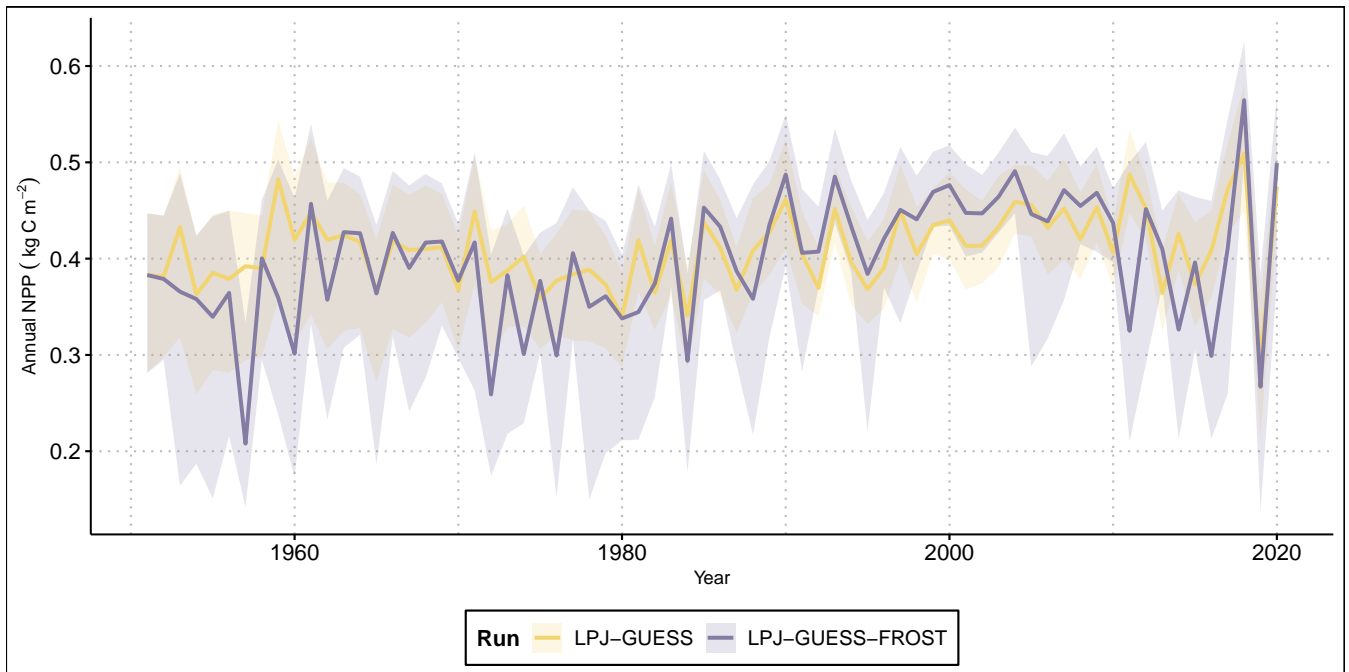
Figure 2. Time series of annual net primary productivity (NPP) from LPJ-GUESS and LPJ-GUESS-FROST. The solid lines show the mean NPP across all 2866 gridcells. The shaded areas contain the 95th percentile range of NPP. Note that due to lower NPP caused by LSF in LPJ-GUESS-FROST, biomass is lower leading to a decrease in maintenance respiration. In none frost years the effect of lower maintenance respiration can lead to higher NPP in LPJ-GUESS-FROST than in LPJ-GUESS.

percent lower than in non-frost years. Averaged across ~~all gridcells~~the entirety of Bavaria, the cumulative reductions
280 in NPP caused by LSF resulted in ~~1.28~~0.79 kg C m^{-2} of lost net productivity by the end of the simulation period in 2020 (Figure 3 A).

The lost productivity translates to biomass loss. By 2020 the effects of LSF result in a mean loss of ~~0.3~~0.57 kg m^{-2}
in vegetation carbon. For the 95th percentile of simulated gridcells the change in vegetation carbon by the end of the
simulation in 2020 ranges from a loss of ~~1.04~~1.22 kg m^{-2} to a gain of ~~0.39~~0.07 kg m^{-2} (Figure 3 B). This biomass
285 loss primarily affects the sapwood which accounts for ~~0.32~~0.38 kg m^{-2} of lost vegetation carbon by 2020 (Figure 3 C).

The modeled biomass loss is in agreement with regional altitudinal patterns across Bavaria: regional maxima of biomass loss are concentrated in low-mountain areas in the south (alpine foothills), south-east (Bavarian Forest), and northern parts (Franconian Jura) of Bavaria (Figure 4).
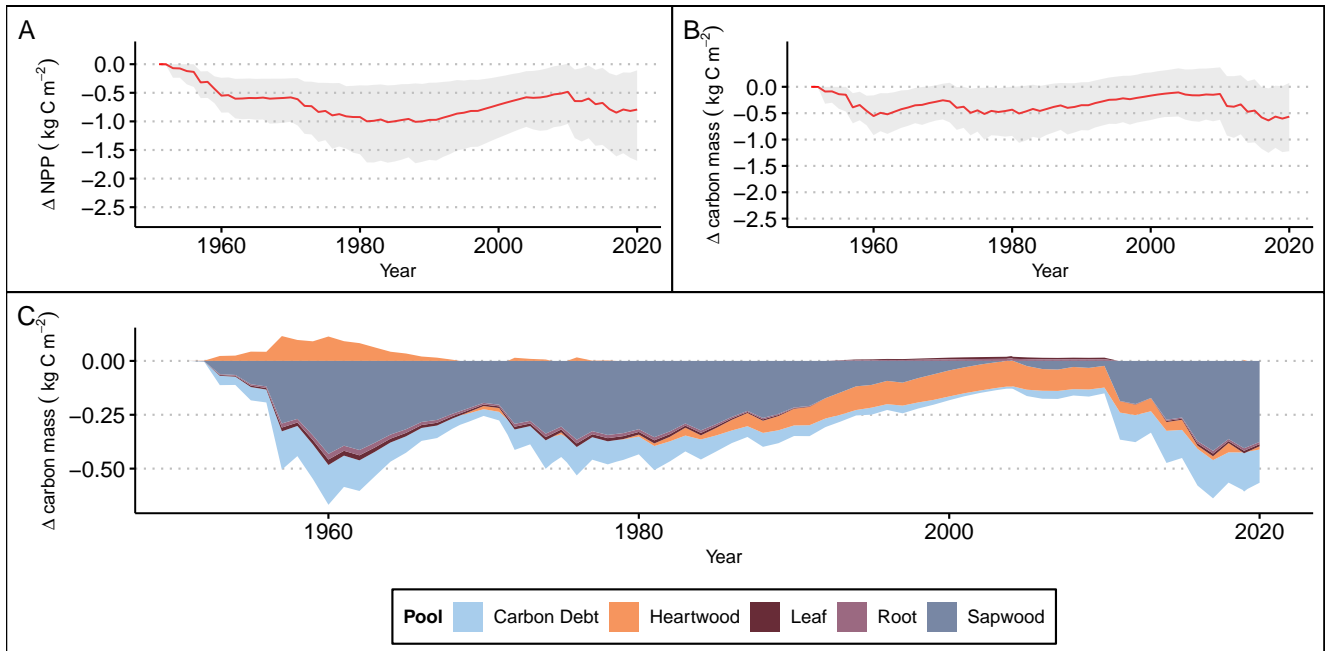
Figure 3. A) Cumulative differences in NPP between LPJ-GUESS-FROST and LPJ-GUESS due to late-frost impacts. The red line represents the mean cumulative NPP difference across all 2866 gridcells. The shaded area contains the 95th percentile range of cumulative NPP differences. B) Differences in total vegetation carbon biomass due to late-frost impacts. The red line shows the difference in mean carbon mass (in kg per square meter) between LPJ-GUESS-FROST and LPJ-GUESS across all 2866 gridcells. The shaded area contains the 95th percentile of range of carbon mass. C) Depiction of each tissue pool's contribution to the total difference in vegetation carbon biomass between LPJ-GUESS-FROST and LPJ-GUESS.

4   Discussion

Using our novel implementation of late-spring frost dynamics in LPJ-GUESS (coined LPJ-GUESS-FROST) we managed to simulate the observed effect of two distinct frost events across large regions of Bavaria (Figure 1). In both LSF years (1953 and 2011), the results from LPJ-GUESS-FROST match the RWI based observations of variability in productivity in showing a distinct negative impact of LSF. ~~While~~ There are no significant differences between the model and observations ~~show no significant differences for~~ for both the 1953 ~~LSF, the model overestimates the damage due to the~~ and 2011 ~~event~~LSF. Notably, however, LPJ-GUESS-FROST simulates a more heterogenous frost response in 1953 than in 2011. This residual difference in responses of LPJ-GUESS-FROST in 1953 and 2011 can be explained by the simulated onset of bud-burst in those years. In 2011, the simulated onset of bud-burst across the 14 sites that experienced LSF ranged from DOY 111 (April 21) to DOY 116 (April 26), well before LSF occurred between DOY 123 (May 3) and DOY 125 (May 5). Subsequently, from a phenological perspective trees at all 14
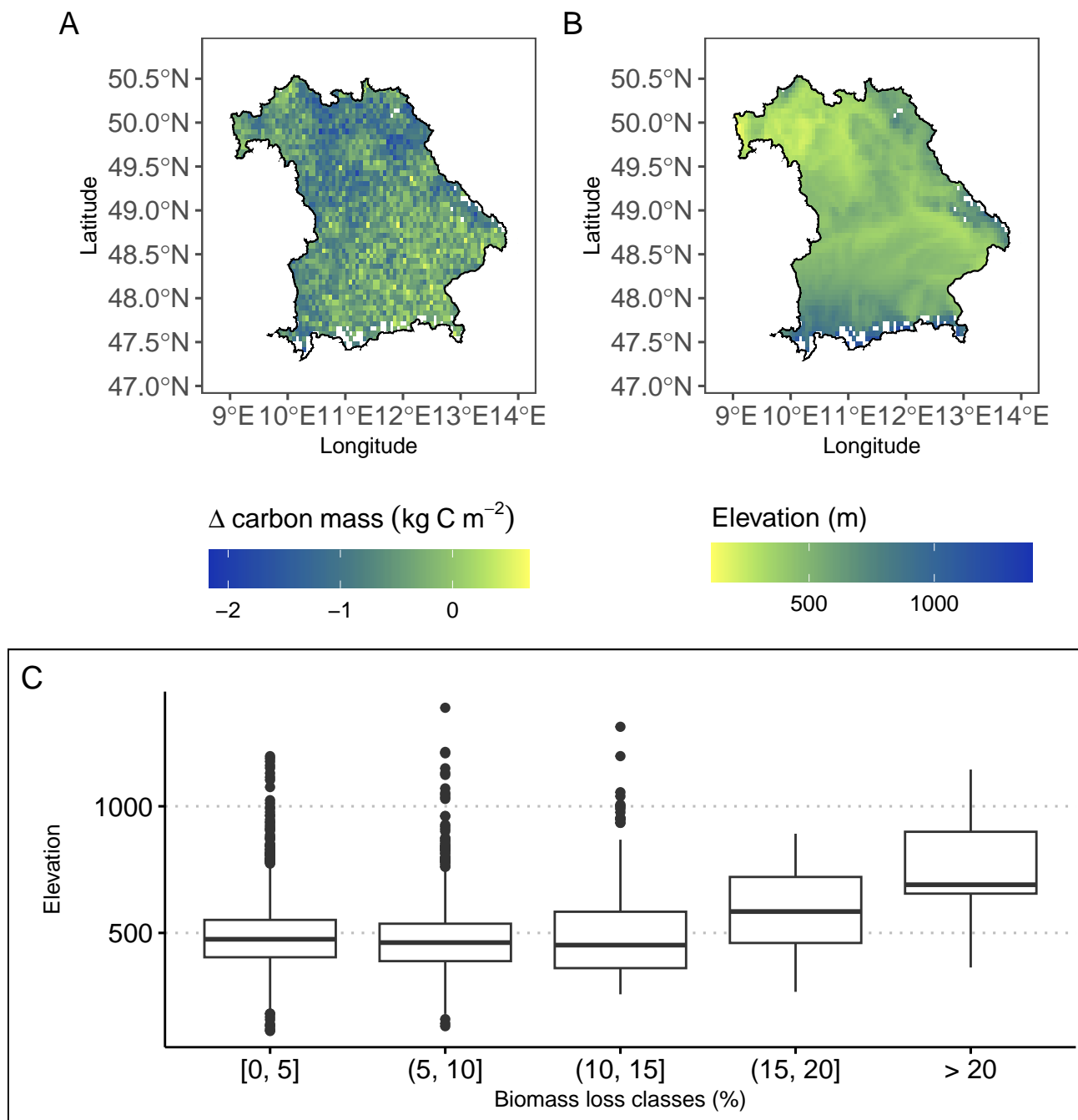
Figure 4. A) Map showing the regional effects of late-frost on whole-tree biomass loss by the end of the simulation period (2020). The heaviest losses with up to ~25% loss of biomass due to LSF were simulated in low-mountain regions across Bavaria (alpine foothills, Bavarian Forest, Franconian Jura) as indicated by the elevation map (based on data from Copernicus DEM (European Space Agency)) (B). C) The highest biomass losses (expressed in percentage loss compared to simulation without frost) tended to occur at higher elevations. On the contrary, low biomass losses are more evenly spread across all elevations.

sites were at risk of frost damage between DOY 123 and DOY 125. In contrast, in 1953 the simulated bud-burst across the 12 sites affected by LSF varied across a larger range from DOY 117 (April 27) to DOY 142 (May 22). The recorded LSF took place between DOY 128 (May 8) and DOY 131 (May 11). At 3 sites, simulated bud-burst occurred after DOY 131, meaning that of the 12 sites only 9 were phenologically predisposed to frost damage in 1953.

While the modeled responses to LSF are not significantly different from the observations, some differences remain. Discrepancies between the model output and the observational data as exhibited by the (e.g., differences in range of modeled and observed responses in 2011LSF) are to be expected. Firstly, we used gridded climate data to drive LPJ-GUESS-FROST which almost certainly does not capture the actual, local temperatures experienced by the sampled trees in either 1953 or 2011 as measured 2m air temperature often deviates from canopy temperature during cold, clear nights (Kollas et al., 2014b). Secondly, while ring-width indices have been shown to be a good proxy for annual variation in NPP, some mismatch between the two metrics must be expected (Xu et al., 2017) due to differences in the demographic structure between modeled and observed tree stands. Nevertheless, our results demonstrate the efficacy of LPJ-GUESS-FROST at simulating the real-life impact of LSF on European beech productivity. Aside from reproducing the impact of the two, well-known frost events for which tree-ring data was available, LPJ-GUESS-FROST simulates several additional LSF across Bavaria suggesting that LSF is not a rare phenomenon in beech forests. Anecdotal evidence from agricultural observations confirms occurrence of LSF in a number of the years simulated as LSF years by LPJ-GUESS-FROST (e.g., 2014, 2016, 2019) (https://www.lwg.bayern.de/weinbau/087592/index.php, https://www.wetteronline.de/extremwetter/eisige-naechte-mitten-im-april-millionenschaeden-nach-spaetfrost-2017-04-24-fa)

SubsequentlyConsequently, LPJ-GUESS-FROST enables us to show the potential extent of losses in productivity and biomass due to frost damage (Figure 3). Frost damage consistently led to lower productivity across large regions of Bavaria. Roughly 30% of GPP and nearly 50% of NPP was lost to frost damage in years with late-frost. This matches results from Urbanski et al. (2007) who found a severe anomaly in net ecosystem exchange (40% of 13 year mean) following a late-frost event in Harvard Forest in 1998. In contrastSimilarly, remote sensing analysis of a LSF event in the northeastern USA in 2010 indicated a 7-14 % decrease in gross ecosystem productivity due to frost damage (Hufkens et al., 2012). It is important to note that the remote sensing approach used by Hufkens et al. (2012) necessarily includes information on all tree species in the study region. On the other hand, our simulations were specifically tailored to identify the impact of late-frost on a single species, *Fagus sylvatica*. Therefore a mismatch in productivity losses between the two studies is to be expected. The regional assessment done by Hufkens et al. (2012) included an early leafing species, sugar maple, and two species with later leaf-out, American beech and yellow birch. Accordingly sugar maples were most affected by frost-damage. The lesser affected species may in turn have buffered some of the productivity response to frost. These dynamics are absent from our study as we focused solely

on simulating ~~European beech monocultures~~monospecific European beech stands. While this does not represent the current state of Bavarian forests which ~~are currently~~ until recently have been heavily managed to favor coniferous species for wood production (Kenk and Guehne, 2001; Schütz, 1999), historically central European ~~forest~~ forests were dominated by beech (Ellenberg et al., 2010). As management efforts increasingly aim to re-institute large shares of beech (Kenk and Guehne, 2001) our aim is to highlight the potential effect of LSF on productivity dynamics in beech forests.

Additionally, we were able to simulate the extent to which losses in primary productivity translate to losses in tree biomass (Figure 3). The majority of simulated biomass losses stem from reduction in sapwood biomass. This behavior is consistent with observed late-frost damage in tree-rings where frost-damaged trees displayed smaller sapwood increments than their non-damaged counterparts (Rubio-Cuadrado et al., 2021). Frost damage primarily manifests as a disruption of the photosynthetic apparatus via partial or full canopy defoliation (Menzel et al., 2015; Inouye, 2000). Following defoliation, affected trees must recover their canopy before full photosynthetic activity can resume, effectively shortening their growing season (Augspurger, 2009). The additive effects of a shorter growing season and re-allocation of stored reserves (D'Andrea et al., 2019) to the new canopy consequently contribute to reduced radial growth in frost years. We capture part of this process by implementing a leafless period after LSF in LPJ-GUESS-FROST. After late-frost induced canopy defoliation occurs in the model the simulated phenology remains dormant for an extended period (see Menzel et al., 2015; Rubio-Cuadrado et al., 2021; Nolè et al., 2018). The absence of leaves in the model prohibits photosynthesis and ultimately reduces the simulated annual NPP consistent with observations.

While we are able to compare our simulated productivity losses with those estimated by Hufkens et al. (2012) and Urbanski et al. (2007), to the best of our knowledge no previous study has quantified the effect of late-frost on tree biomass. This would require forest stands with identical environmental conditions aside from late-frost, which is not possible in a natural setting but can be simulated using DVMs. We show that the impact of LSF on carbon storage in plant biomass in European beech forests is non-negligible. ~~Within the 69 years of our simulation experiment, LSF caused a five percent reduction~~ In the final year of our 69-year simulation period the difference in vegetation carbon ~~compared to a simulation without~~ between LPJ-GUESS and LPJ-GUESS-FROST amounted to a five percent reduction due to the effects of LSF. To put this in context, Lindeskog et al. (2021) found that accounting for thinning in LPJ-GUESS yielded a reduction in vegetation carbon of 3% to 5% across Europe until 2010, compared to a simulation without thinning suggesting that the effect of LSF on tree biomass can have a substantial effect on forest structure and functioning.

Nevertheless, these results must be interpreted with some caution. The implementation of late-spring frost in LPJ-GUESS-FROST is intended to provide potential estimates of frost induced shifts in carbon dynamics. In reality, LSF is a highly localized disturbance, dependent on a forest stand's microclimate and frost tolerance. Accounting for these two factors introduces stochasticity into the frost scheme of LPJ-GUESS-FROST. Currently, LPJ-GUESS-FROST

cannot simulate microclimate. While replicate patches are used to abstract forest structure, this is not the case for climate which is constant across all patches in a gridcell. In addition, the frost tolerance of European beech leaves is a point of contention. Studies directly applying freezing temperatures to twig samples have found frost tolerance for European beech to range from -4.8°C to -6.4°C at and directly following budburst (Lenz et al., 2013, 2016; Vitra et al., 2017). These results conflict with observations of frost damage in European beech stands where recorded ambient temperatures from nearby climate stations were significantly higher. In fact, frost damage in European beech has been observed at temperatures as high as -1.2°C (Príncipe et al., 2017) and evidence from remote-sensing of LSF suggests canopy decline may already occur at -1°C (Buras et al., 2021). Similarly, -2.2°C is a commonly accepted, species agnostic temperature threshold for palpable frost risk (Chamberlain et al., 2019; Schwartz, 1993). This discrepancy is caused by the effect of radiative cooling. During clear, windless nights the temperature at the leaf tissue, where frost damage occurs, can potentially be several degrees lower than the ambient air temperature measured at climate stations (Matsui et al., 1981; Neuner, 2014). To overcome these problems we inverted the mechanism determining frost occurrence. Since we cannot meaningfully model microclimate on a patch level and there is uncertainty in the specific frost threshold of leaves, we instead decided to model the frost threshold as stochastically variable at the patch level. In this manner we approximate the local differences in frost occurrence while simultaneously accounting for the lack of an accurate frost threshold. While this abstraction approximates the real-world heterogeneity inherent to LSF, it is stochastic in nature. Therefore, the intensity of simulated frost damage may not always match observations.

4.1 Conclusions and Outlook

Our results indicate the importance of including late-spring frost dynamics in DVMs. We demonstrate that known patterns of productivity loss in European beech due to LSF can be reproduced by LPJ-GUESS-FROST. Additionally, we found that LSF leads to distinct regional variation in simulated biomass loss and influences the allocation of carbon within individual trees. While these findings are relevant in their own right they also imply a need to focus future research efforts on identifying the implications of LSF across multiple tree species and climate change scenarios. To do this, further modeling efforts in the realm of LSF should attempt to simulate microclimate within stands, or at the very least, develop routines to accurately account for the discrepancy between measured 2m air temperature and leaf temperature due to radiative cooling. Considering that the commonly used forcing from GCM outputs is quite coarse and therefore unlikely to capture such localized effects, this poses a particular challenge for modeling future dynamics. Additionally, due to the strong controls of leaf-out on frost risk (Vitasse et al., 2014; Ma et al., 2019), improving the phenological models used in LPJ-GUESS(-FROST) should be a priority. Aside from parameterizing the phenological model for a wide range of broadleaved, deciduous species (e.g., maple, hornbeam, ash, etc.), future phenology routines should also consider age-dependent variation in bud-burst times. Similarly, while we demonstrate that accounting for loss of photosynthetic capacity due to defoliation can simulate productivity losses that are comparable to observations, the ~~carbon costs for~~ relatively simple representation of carbon costs related to LSF

damage and subsequent canopy re-building ~~the canopy should not be ignored~~leaves room for improvement. Here, the integration of explicitly modeled non-structural carbohydrates into LPJ-GUESS-FROST could pave the way for a better representation of LSF impacts.

Appendix A

A1: Frost threshold sensitivity analysis
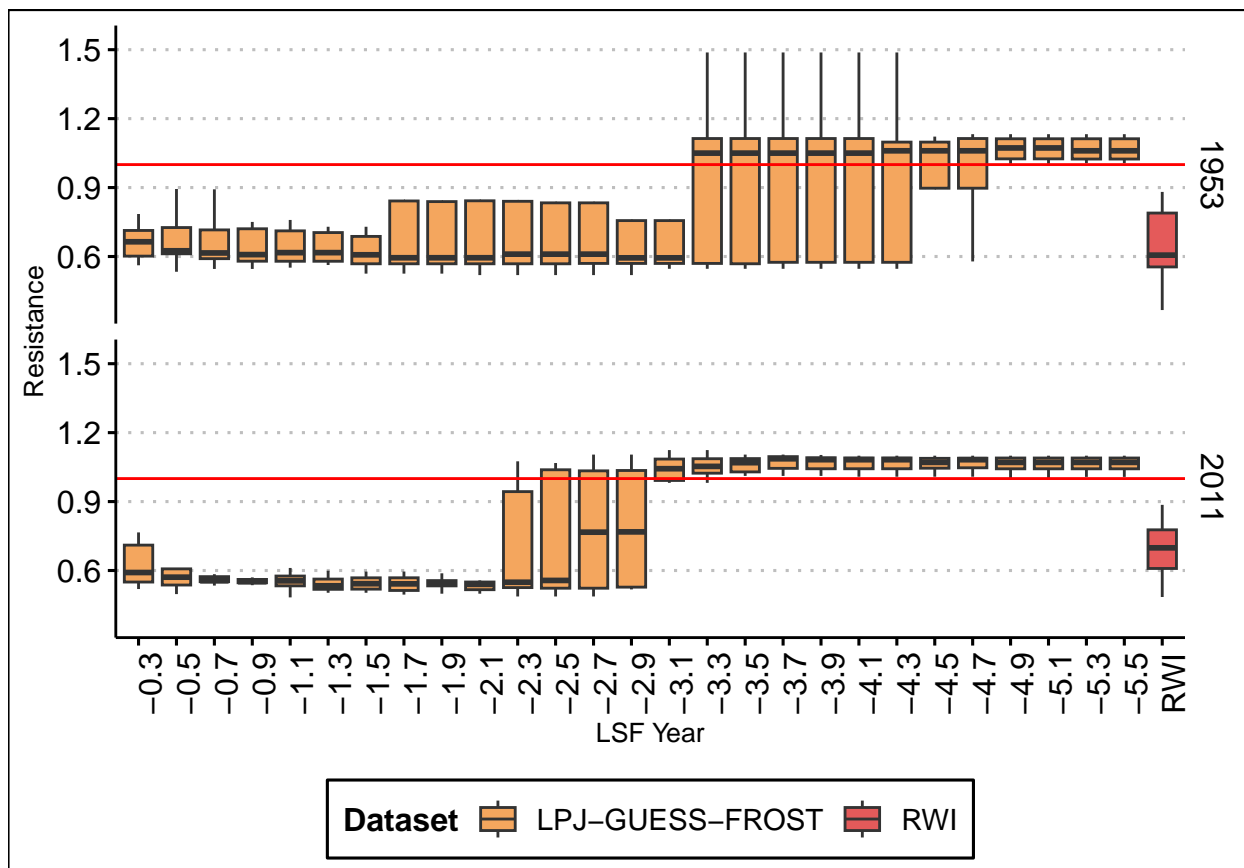
Figure A1. Sensitivity analysis to determine the range of the frost threshold. For both known frost years we ran simulations for LPJ-GUESS-FROST with varying frost threshold temperatures from -0.3°C to -5.5°C. We then computed the resistance index (see Methods) for each simulation and for the RWI-based observations. To determine $T_{frost_{mu}}$ and $T_{frost_{sigma}}$ we discarded all frost thresholds which resulted in a median resistance greater than 1 (i.e. higher productivity in frost year than in pre-frost years) and computed the mean and standard deviation of the remaining thresholds (mean = -1.65, standard deviation = 0.85). The boxplots show the median resistance, quartiles, and 1.5 interquartile range. The solid, red line indicates a resistance of 1.
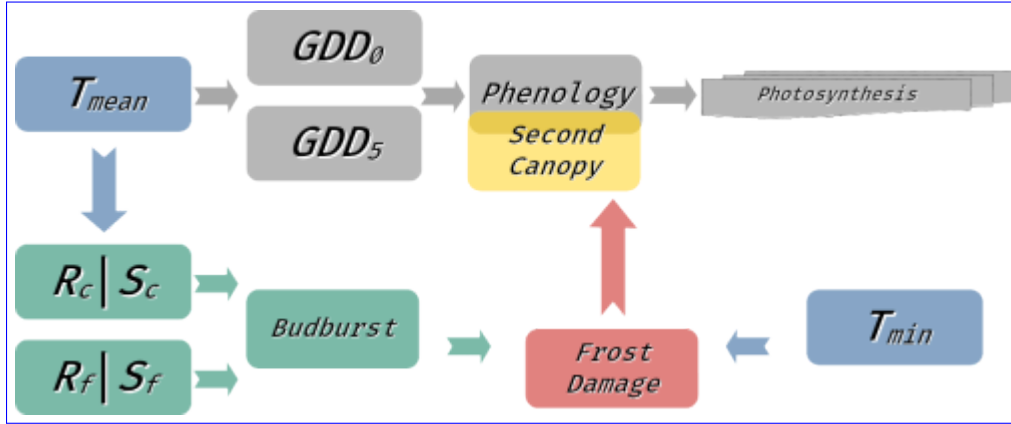
Figure A2. Schematic showing the integration of the new frost module (red, green, and yellow) with the existing LPJ-GUESS phenology model (grey) in dependence on climatic drivers (blue). The LPJ-GUESS growing degree day model (Equations 1-2 in the Methods section) simulates continuous leaf development from 0 (no leaves) to 1 (full canopy cover). This phenological status is then used for further model processes such as photosynthesis. The new frost module includes a parallel phenological bud-burst model which simulates a distinct point of bud-burst (i.e. the point at which developing leaves become sensitive to LSF). This model uses a sequential, two-stage approach with a chilling stage (Rc,Sc) and a forcing stage (Rf,Sf) described in Equations 3-6 in the methods section. This bud-burst status is used to determine LSF damage in conjunction with the minimum temperature (Tmin). In the case of LSF, the continuous phenological status is reset to 0 and a second cohort of leaves has to be rebuilt before photosynthetic activity can resume.
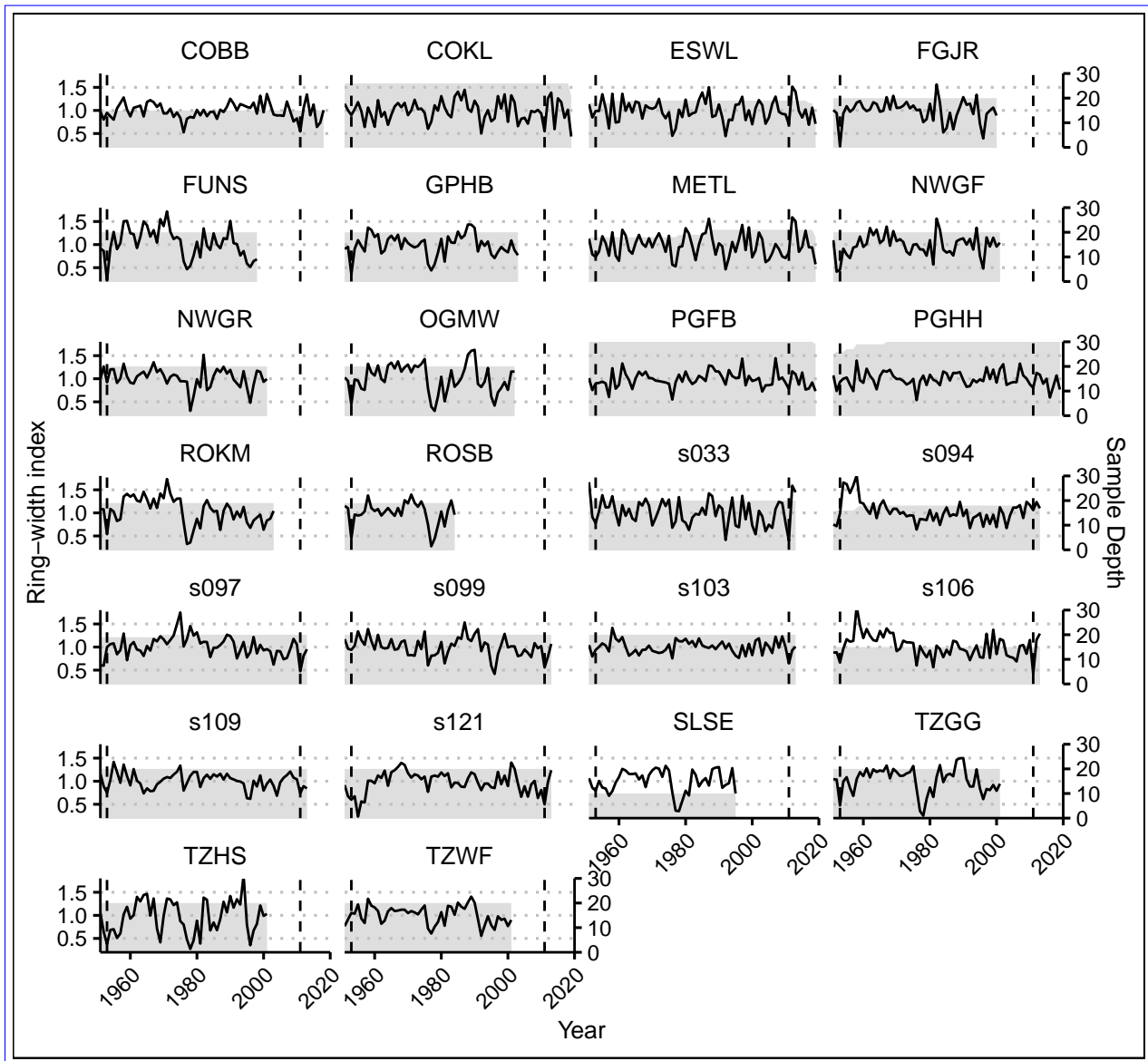
Figure A3. Spline detrended tree-ring chronologies per site. The solid black line depicts the mean chronology of ring-width indices (left y-axis) and the grey, shaded area signifies the number of individual tree-ring series contained in the mean chronology in any given year (right y-axis). The dashed, vertical lines indicate the LSF in 1953 and 2011.
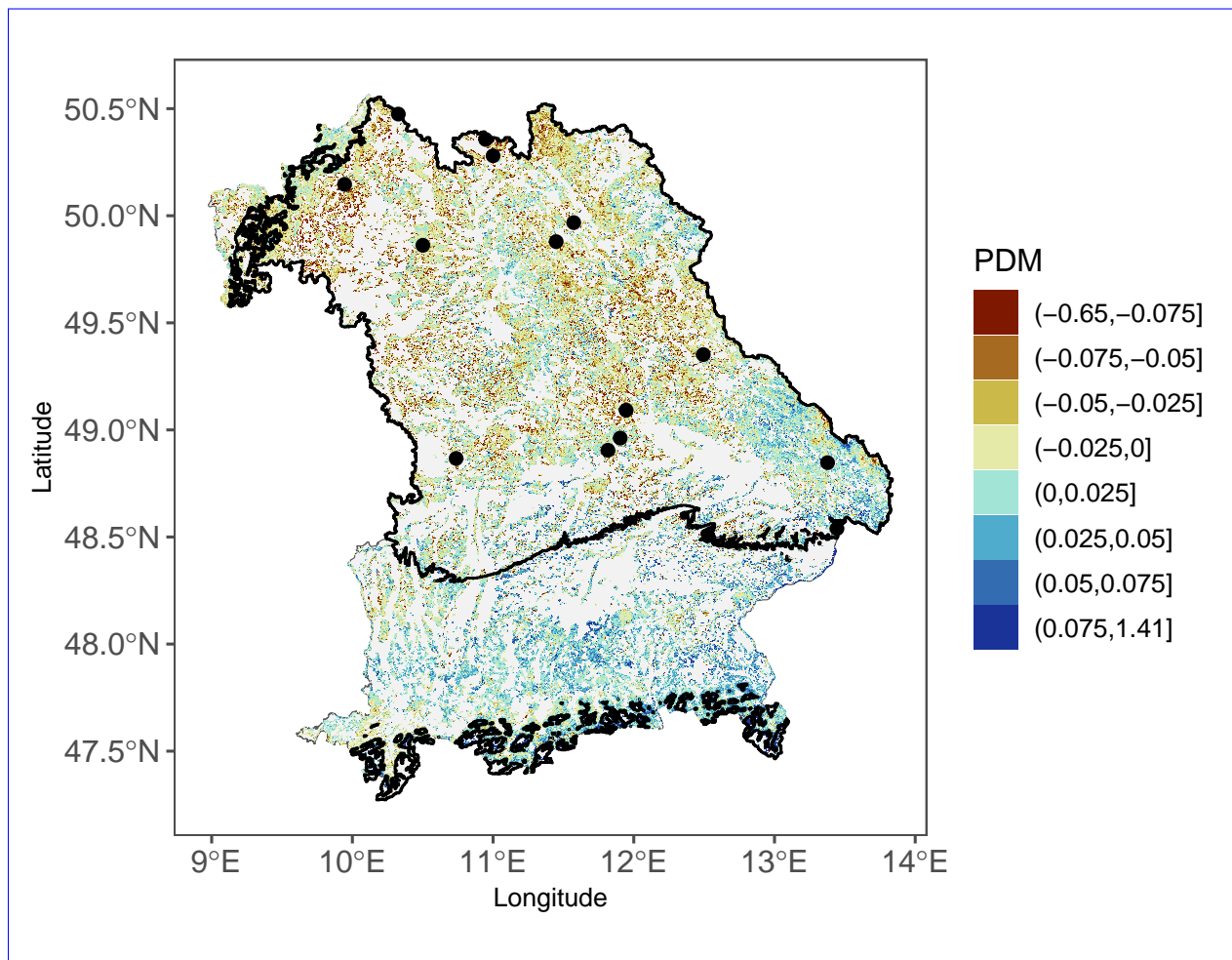
Figure A4. Map of proportional deviations from the median from the EFCM for the 2011 LSF. The black line indicates the area which experienced temperatures below -1.65°C on May 4th, 2011. The black dots show the tree-ring sites affected by LSF in 2011.

Code and data availability. LPJ-GUESS v4.0.1 is openly accessible and available at https://doi.org/10.5281/zenodo.8070582. The modified version of LPJ-GUESS used in this study is openly accessible and available at https://zenodo.org/doi/10.5281/zenodo.10562597. The data analysis pipeline to reproduce the results and figures from this study is openly accessible and available at https://zenodo.org/doi/10.5281/zenodo.10564746. All data needed to reproduce the analysis are openly accessible and

415   available at https://zenodo.org/doi/10.5281/zenodo.10562678.

Author contributions. BM, CZ, and AB conceived the study. BM performed the data analysis and model runs and prepared the manuscript. CZ, AB, AP, and JK contributed data. KG, LL, and AR contributed input to the model development. All authors contributed input to paper writing and revisions.

Competing interests. One of the (co-)authors is a member of the editorial board of Biogeosciences. The peer-review process

420   was guided by an independent editor, and the authors have no other competing interests to declare.

Acknowledgements. This project is funded by the Bavarian Ministry of Science and the Arts in the context of the Bavarian Climate Research Network (BayKliF). We sincerely thank Christoph Dittmar for providing and allowing us to publish the tree ring data from Dittmar et al. (2006) used in this study. We thank Anja Žmegač for preparing, dating, and measuring the newly sampled tree cores used in this study.

References

Anderegg, W. R. L., Trugman, A. T., Badgley, G., Konings, A. G., and Shaw, J.: Divergent Forest Sensitivity to Repeated Extreme Droughts, Nature Climate Change, 10, 1091–1095, https://doi.org/10.1038/s41558-020-00919-1, 2020.

Arnold, J. B.: Ggthemes: Extra Themes, Scales and Geoms for 'Ggplot2', 2021.

Arya, S., Mount, D., Kemp, S. E., and Jefferis, G.: RANN: Fast Nearest Neighbour Search (Wraps ANN Library) Using L2 Metric, 2019.

Augspurger, C. K.: Spring 2007 Warmth and Frost: Phenology, Damage and Refoliation in a Temperate Deciduous Forest, Functional Ecology, 23, 1031–1039, https://doi.org/10.1111/j.1365-2435.2009.01587.x, 2009.

Bauer, D. F.: Constructing Confidence Sets Using Rank Statistics, Journal of the American Statistical Association, 67, 687–690, https://doi.org/10.1080/01621459.1972.10481279, 1972.

Bayerisches Landesamt für Umwelt [Hrsg.]: Bayerische Klimadaten - Beobachtungsdaten, Klima- Projektionsensemble Und Klimakennwerte Für Bayern, 2020.

Bhuyan, U., Zang, C., and Menzel, A.: Different Responses of Multispecies Tree Ring Growth to Various Drought Indices across Europe, Dendrochronologia, 44, 1–8, https://doi.org/10.1016/j.dendro.2017.02.002, 2017.

Bohn, U. and Welß, W.: Die Potenzielle Natürliche Vegetation, Klima, Pflanzen-Und Tierwelt. In: Leibnitz-Institut für Länderkunde [hrsg.]: Nationalatlas Bundesrepublik Deutschland, 3, 84–87, 2003.

Bolte, A., Ammer, C., Löf, M., Madsen, P., Nabuurs, G.-J., Schall, P., Spathelf, P., and Rock, J.: Adaptive Forest Management in Central Europe: Climate Change Impacts, Strategies and Integrative Concept, Scandinavian Journal of Forest Research, 24, 473–482, https://doi.org/10.1080/02827580903418224, 2009.

Bonan, G. B.: Forests and Climate Change: Forcings, Feedbacks, and the Climate Benefits of Forests, Science, 320, 1444–1449, https://doi.org/10.1126/science.1155121, 2008.

Bunn, A., Korpela, M., Biondi, F., Campelo, F., Mérian, P., Qeadan, F., and Zang, C.: dplR: Dendrochronology Program Library in R, 2022.

Buras, A., Rammig, A., and Zang, C. S.: The European Forest Condition Monitor: Using Remotely Sensed Forest Greenness to Identify Hot Spots of Forest Decline, Frontiers in Plant Science, 12, 2021.

Chamberlain, C. J. and Wolkovich, E. M.: Late Spring Freezes Coupled with Warming Winters Alter Temperate Tree Phenology and Growth, New Phytologist, 231, 987–995, https://doi.org/10.1111/nph.17416, 2021.

Chamberlain, C. J., Cook, B. I., García de Cortázar-Atauri, I., and Wolkovich, E. M.: Rethinking False Spring Risk, Global Change Biology, 25, 2209–2220, https://doi.org/10.1111/gcb.14642, 2019.

Chen, L., Keski-Saari, S., Kontunen-Soppela, S., Zhu, X., Zhou, X., Hänninen, H., Pumpanen, J., Mola-Yudego, B., Wu, D., and Berninger, F.: Immediate and Carry-over Effects of Late-Spring Frost and Growing Season Drought on Forest Gross Primary Productivity Capacity in the Northern Hemisphere, Global Change Biology, 29, 3924–3940, https://doi.org/10.1111/gcb.16751, 2023.

Cook, E. R.: The Decomposition of Tree-Ring Series for Environmental Studies, 1987.

Cook, E. R. and Peters, K.: Calculating Unbiased Tree-Ring Indices for the Study of Climatic and Environmental Change, The Holocene, 7, 361–370, https://doi.org/10.1177/095968369700700314, 1997.

D'Andrea, E., Rezaie, N., Battistelli, A., Gavrichkova, O., Kuhlmann, I., Matteucci, G., Moscatello, S., Proietti, S., Scartazza, A., Trumbore, S., and Muhr, J.: Winter's Bite: Beech Trees Survive Complete Defoliation Due to Spring Late-Frost Damage by Mobilizing Old c Reserves, New Phytol, 224, 625–631, https://doi.org/10.1111/nph.16047, 2019.

Dittmar, C., Fricke, W., and Elling, W.: Impact of Late Frost Events on Radial Growth of Common Beech (Fagus Sylvatica l.) in Southern Germany, European Journal of Forest Research, 125, 249–259, https://doi.org/10.1007/s10342-005-0098-y, 2006.

Douglas Nychka, Reinhard Furrer, John Paige, and Stephan Sain: Fields: Tools for Spatial Data, 2021.

Dulamsuren, C., Hauck, M., Kopp, G., Ruff, M., and Leuschner, C.: European Beech Responds to Climate Change with Growth Decline at Lower, and Growth Increase at Higher Elevations in the Center of Its Distribution Range (SW Germany), Trees, 31, 673–686, https://doi.org/10.1007/s00468-016-1499-x, 2017.

Duveneck, M. J. and Thompson, J. R.: Climate Change Imposes Phenological Trade-Offs on Forest Net Primary Productivity, Journal of Geophysical Research: Biogeosciences, 122, 2298–2313, https://doi.org/10.1002/2017JG004025, 2017.

Ellenberg, H., Leuschner, C., and Dierschke, H.: Vegetation Mitteleuropas mit den Alpen: in ökologischer, dynamischer und historischer Sicht ; 203 Tabellen, no. 8104 in UTB Botanik, Ökologie, Agrar- und Forstwissenschaften, Geographie, Verlag Eugen Ulmer, Stuttgart, 6., vollständig neu bearbeitete und stark erweiterte auflage edn., 2010.

European Space Agency: Copernicus DEM, https://doi.org/10.5270/ESA-c5d3d65.

Firke, S.: Janitor: Simple Tools for Examining and Cleaning Dirty Data, 2021.

Gampe, D., Zscheischler, J., Reichstein, M., O'Sullivan, M., Smith, W. K., Sitch, S., and Buermann, W.: Increasing Impact of Warm Droughts on Northern Ecosystem Productivity over Recent Decades, Nature Climate Change, 11, 772–779, https://doi.org/10.1038/s41558-021-01112-8, 2021.

Gazol, A., Camarero, J. J., Colangelo, M., de Luis, M., Martínez del Castillo, E., and Serra-Maluquer, X.: Summer Drought and Spring Frost, but Not Their Interaction, Constrain European Beech and Silver Fir Growth in Their Southern Distribution Limits, Agricultural and Forest Meteorology, 278, 107 695, https://doi.org/10.1016/j.agrformet.2019.107695, 2019.

Graves, S., Piepho, H.-P., and Dorai-Raj, L. S. w. h. f. S.: multcompView: Visualizations of Paired Comparisons, 2019.

Grossman, J. J.: Phenological Physiology: Seasonal Patterns of Plant Stress Tolerance in a Changing Climate, New Phytologist, 237, 1508–1524, https://doi.org/10.1111/nph.18617, 2023.

Hickler, T., Smith, B., Sykes, M. T., Davis, M. B., Sugita, S., and Walker, K.: Using a Generalized Vegetation Model to Simulate Vegetation Dynamics in Northeastern USA, Ecology, 85, 519–530, https://doi.org/10.1890/02-0344, 2004.

Hickler, T., Vohland, K., Feehan, J., Miller, P. A., Smith, B., Costa, L., Giesecke, T., Fronzek, S., Carter, T. R., Cramer, W., Kühn, I., and Sykes, M. T.: Projecting the Future Distribution of European Potential Natural Vegetation Zones with a Generalized, Tree Species-Based Dynamic Vegetation Model: Future Changes in European Vegetation Zones, Global Ecology and Biogeography, 21, 50–63, https://doi.org/10.1111/j.1466-8238.2010.00613.x, 2012.

Hijmans, R. J.: Terra: Spatial Data Analysis, 2022.

Hufkens, K., Friedl, M. A., Keenan, T. F., Sonnentag, O., Bailey, A., O'Keefe, J., and Richardson, A. D.: Ecological Impacts of a Widespread Frost Event Following Early Spring Leaf-Out, Global Change Biology, 18, 2365–2377, https://doi.org/10.1111/j.1365-2486.2012.02712.x, 2012.

Inouye, D.: The Ecological and Evolutionary Significance of Frost in the Context of Climate Change, Ecology Letters, 3, 457–463, https://doi.org/10.1046/j.1461-0248.2000.00165.x, 2000.

Jevšenak, J.: Daily Climate Data Reveal Stronger Climate-Growth Relationships for an Extended European Tree-Ring Network, Quaternary Science Reviews, 221, 105 868, https://doi.org/10.1016/j.quascirev.2019.105868, 2019.

500   Keenan, T. F., Gray, J., Friedl, M. A., Toomey, M., Bohrer, G., Hollinger, D. Y., Munger, J. W., O'Keefe, J., Schmid, H. P., Wing, I. S., Yang, B., and Richardson, A. D.: Net Carbon Uptake Has Increased through Warming-Induced Changes in Temperate Forest Phenology, Nature Climate Change, 4, 598–604, https://doi.org/10.1038/nclimate2253, 2014.

Kenk, G. and Guehne, S.: Management of Transformation in Central Europe, Forest Ecology and Management, 151, 107–119, https://doi.org/10.1016/S0378-1127(00)00701-5, 2001.

505   Kollas, C., Körner, C., and Randin, C. F.: Spring Frost and Growing Season Length Co-Control the Cold Range Limits of Broad-Leaved Trees, Journal of Biogeography, 41, 773–783, https://doi.org/10.1111/jbi.12238, 2014a.

Kollas, C., Randin, C. F., Vitasse, Y., and Körner, C.: How Accurately Can Minimum Temperatures at the Cold Limits of Tree Species Be Extrapolated from Weather Station Data?, Agricultural and Forest Meteorology, 184, 257–266, https://doi.org/10.1016/j.agrformet.2013.10.001, 2014b.

510   Körner, C., Basler, D., Hoch, G., Kollas, C., Lenz, A., Randin, C. F., Vitasse, Y., and Zimmermann, N. E.: Where, Why and How? Explaining the Low-Temperature Range Limits of Temperate Tree Species, Journal of Ecology, 104, 1076–1088, https://doi.org/10.1111/1365-2745.12574, 2016.

Kramer, K., Ducousso, A., Gömöry, D., Hansen, J. K., Ionita, L., Liesebach, M., Lorenţ, A., Schüler, S., Sulkowska, M., de Vries, S., and von Wühlisch, G.: Chilling and Forcing Requirements for Foliage Bud Burst of European Beech (Fagus
515   Sylvatica L.) Differ between Provenances and Are Phenotypically Plastic, Agricultural and Forest Meteorology, 234–235, 172–181, https://doi.org/10.1016/j.agrformet.2016.12.002, 2017.

Lenz, A., Hoch, G., Vitasse, Y., and Körner, C.: European Deciduous Trees Exhibit Similar Safety Margins against Damage by Spring Freeze Events along Elevational Gradients, New Phytologist, 200, 1166–1175, https://doi.org/10.1111/nph.12452, 2013.

520   Lenz, A., Hoch, G., Körner, C., and Vitasse, Y.: Convergence of Leaf-out towards Minimum Risk of Freezing Damage in Temperate Trees, Functional Ecology, 30, 1480–1490, https://doi.org/10.1111/1365-2435.12623, 2016.

Lindeskog, M., Arneth, A., Miller, P., Nord, J., Mischurov, M., Olin, S., Schurgers, G., Smith, B., Wårlind, D., and And Past LPJ-GUESS Contributors: LPJ-GUESS Release v4.0.1 Model Code, Zenodo, https://doi.org/10.5281/ZENODO.8070582, 2017.

525   Lindeskog, M., Smith, B., Lagergren, F., Sycheva, E., Ficko, A., Pretzsch, H., and Rammig, A.: Accounting for Forest Management in the Estimation of Forest Carbon Balance Using the Dynamic Vegetation Model LPJ-GUESS (v4.0, R9710): Implementation and Evaluation of Simulations for Europe, Geoscientific Model Development, 14, 6071–6112, https://doi.org/10.5194/gmd-14-6071-2021, 2021.

Liu, Q., Piao, S., Janssens, I. A., Fu, Y., Peng, S., Lian, X., Ciais, P., Myneni, R. B., Peñuelas, J., and Wang, T.: Extension of the
530   Growing Season Increases Vegetation Exposure to Frost, Nature Communications, 9, 426, https://doi.org/10.1038/s41467-017-02690-y, 2018.

Lloret, F., Keeling, E. G., and Sala, A.: Components of Tree Resilience: Effects of Successive Low-Growth Episodes in Old Ponderosa Pine Forests, Oikos, 120, 1909–1920, https://doi.org/10.1111/j.1600-0706.2011.19372.x, 2011.

Ma, Q., Huang, J.-G., Hänninen, H., and Berninger, F.: Divergent Trends in the Risk of Spring Frost Damage to Trees in
535   Europe with Recent Warming, Global Change Biology, 25, 351–360, https://doi.org/10.1111/gcb.14479, 2019.

Massicotte, P. and South, A.: rnaturalearth: World map data from natural earth, Tech. rep., https://CRAN.R-project.org/package=rnaturalearth, 2023.

Matsui, T., Eguchi, H., and Mori, K.: Control of Dew and Frost Formations on Leaf by Radiative Cooling, Environment Control in Biology, 19, 51–57, https://doi.org/10.2525/ecb1963.19.51, 1981.

540 Medlyn, B. E., Duursma, R. A., and Zeppel, M. J. B.: Forest Productivity under Climate Change: A Checklist for Evaluating Model Studies, WIREs Climate Change, 2, 332–355, https://doi.org/10.1002/wcc.108, 2011.

Menzel, A., Estrella, N., and Fabian, P.: Spatial and Temporal Variability of the Phenological Seasons in Germany from 1951 to 1996, Global Change Biology, 7, 657–666, https://doi.org/10.1111/j.1365-2486.2001.00430.x, 2001.

Menzel, A., Helm, R., and Zang, C.: Patterns of Late Spring Frost Leaf Damage and Recovery in a European Beech
545 (Fagus Sylvatica l.) Stand in South-Eastern Germany Based on Repeated Digital Photographs, Front. Plant Sci., 6, https://doi.org/10.3389/fpls.2015.00110, 2015.

Meyer, B. F., Buras, A., Rammig, A., and Zang, C. S.: Higher Susceptibility of Beech to Drought in Comparison to Oak, Dendrochronologia, p. 125780, https://doi.org/10.1016/j.dendro.2020.125780, 2020.

Morin, X., Lechowicz, M. J., Augspurger, C., O'keefe, J., Viner, D., and Chuine, I.: Leaf Phenology in 22 North American Tree
550 Species during the 21st Century, Global Change Biology, 15, 961–975, https://doi.org/10.1111/j.1365-2486.2008.01735.x, 2009.

Müller, K.: Here: A Simpler Way to Find Your Files, 2020.

Neuner, G.: Frost Resistance in Alpine Woody Plants, Frontiers in Plant Science, 5, 2014.

Nolè, A., Rita, A., Ferrara, A. M. S., and Borghetti, M.: Effects of a Large-Scale Late Spring Frost on a Beech (Fagus Sylvatica
555 L.) Dominated Mediterranean Mountain Forest Derived from the Spatio-Temporal Variations of NDVI, Annals of Forest Science, 75, https://doi.org/10.1007/s13595-018-0763-1, 2018.

Pebesma, E.: Simple Features for R: Standardized Support for Spatial Vector Data, The R Journal, 10, 439–446, https://doi.org/10.32614/RJ-2018-009, 2018.

Pedersen, T. L.: Patchwork: The Composer of Plots, 2020.

560 Pedersen, T. L. and Crameri, F.: Scico: Colour Palettes Based on the Scientific Colour-Maps, 2022.

Pierce, D.: Ncdf4: Interface to Unidata netCDF (Version 4 or Earlier) Format Data Files, 2022.

Pretzsch, H., Schütze, G., and Uhl, E.: Resistance of European Tree Species to Drought Stress in Mixed versus Pure Forests: Evidence of Stress Release by Inter-Specific Facilitation, Plant Biology, 15, 483–495, https://doi.org/10.1111/j.1438-8677.2012.00670.x, 2013.

565 Príncipe, A., van der Maaten, E., van der Maaten-Theunissen, M., Struwe, T., Wilmking, M., and Kreyling, J.: Low Resistance but High Resilience in Growth of a Major Deciduous Forest Tree (Fagus Sylvatica L.) in Response to Late Spring Frost in Southern Germany, Trees, 31, 743–751, https://doi.org/10.1007/s00468-016-1505-3, 2017.

R Core Team: R: A Language and Environment for Statistical Computing, R Foundation for Statistical Computing, Vienna, Austria, 2022.

570 Rammig, A., Jönsson, A., Hickler, T., Smith, B., Bärring, L., and Sykes, M.: Impacts of Changing Frost Regimes on Swedish Forests: Incorporating Cold Hardiness in a Regional Ecosystem Model, Ecological Modelling, 221, 303–313, https://doi.org/10.1016/j.ecolmodel.2009.05.014, 2010.

Rubio-Cuadrado, Á., Gómez, C., Rodríguez-Calcerrada, J., Perea, R., Gordaliza, G. G., Camarero, J. J., Montes, F., and Gil, L.: Differential Response of Oak and Beech to Late Frost Damage: An Integrated Analysis from Organ to Forest, Agricultural and Forest Meteorology, 297, 108 243, https://doi.org/10.1016/j.agrformet.2020.108243, 2021.

Sangüesa-Barreda, G., Di Filippo, A., Piovesan, G., Rozas, V., Di Fiore, L., García-Hidalgo, M., García-Cervigón, A. I., Muñoz-Garachana, D., Baliva, M., and Olano, J. M.: Warmer Springs Have Increased the Frequency and Extension of Late-Frost Defoliations in Southern European Beech Forests, Science of The Total Environment, 775, 145 860, https://doi.org/10.1016/j.scitotenv.2021.145860, 2021.

Scharnweber, T., Manthey, M., Criegee, C., Bauwe, A., Schröder, C., and Wilmking, M.: Drought Matters – Declining Precipitation Influences Growth of Fagus Sylvatica L. and Quercus Robur L. in North-Eastern Germany, Forest Ecology and Management, 262, 947–961, https://doi.org/10.1016/j.foreco.2011.05.026, 2011.

Schütz, J. P.: Close-to-Nature Silviculture: Is This Concept Compatible with Species Diversity?, Forestry (Lond), 72, 359–366, https://doi.org/10.1093/forestry/72.4.359, 1999.

Schwartz, M. D.: Assessing the Onset of Spring: A Climatological Perspective, Physical Geography, 14, 536–550, https://doi.org/10.1080/02723646.1993.10642496, 1993.

Schwartz, M. D., Ahas, R., and Aasa, A.: Onset of Spring Starting Earlier across the Northern Hemisphere, Global Change Biology, 12, 343–351, https://doi.org/10.1111/j.1365-2486.2005.01097.x, 2006.

Sitch, S., Smith, B., Prentice, I. C., Arneth, A., Bondeau, A., Cramer, W., Kaplan, J. O., Levis, S., Lucht, W., Sykes, M. T., Thonicke, K., and Venevsky, S.: Evaluation of Ecosystem Dynamics, Plant Geography and Terrestrial Carbon Cycling in the LPJ Dynamic Global Vegetation Model, Global Change Biology, 9, 161–185, https://doi.org/10.1046/j.1365-2486.2003.00569.x, 2003.

Smith, B., Prentice, I. C., and Sykes, M. T.: Representation of Vegetation Dynamics in the Modelling of Terrestrial Ecosystems: Comparing Two Contrasting Approaches within European Climate Space: *Vegetation Dynamics in Ecosystem Models*, Global Ecology and Biogeography, 10, 621–637, https://doi.org/10.1046/j.1466-822X.2001.t01-1-00256.x, 2001.

Smith, B., Wårlind, D., Arneth, A., Hickler, T., Leadley, P., Siltberg, J., and Zaehle, S.: Implications of Incorporating N Cycling and N Limitations on Primary Production in an Individual-Based Dynamic Vegetation Model, Biogeosciences, 11, 2027–2054, https://doi.org/10.5194/bg-11-2027-2014, 2014.

South, A., Michael, S., and Massicotte, P.: rnaturalearthhires: High resolution world vector map data from natural earth used in rnaturalearth, Tech. rep., 2024.

Sullivan, P. F., Pattison, R. R., Brownlee, A. H., Cahoon, S. M. P., and Hollingsworth, T. N.: Effect of Tree-Ring Detrending Method on Apparent Growth Trends of Black and White Spruce in Interior Alaska, Environmental Research Letters, 11, 114 007, https://doi.org/10.1088/1748-9326/11/11/114007, 2016.

Sykes, Martint. and Prentice, I.: Climate Change, Tree Species Distributions and Forest Dynamics: A Case Study in the Mixed Conifer/Northern Hardwoods Zone of Northern Europe, Climatic Change, 34, https://doi.org/10.1007/bf00224628, 1996.

Urbanski, S., Barford, C., Wofsy, S., Kucharik, C., Pyle, E., Budney, J., McKain, K., Fitzjarrald, D., Czikowsky, M., and Munger, J. W.: Factors Controlling CO_2 Exchange on Timescales from Hourly to Decadal at Harvard Forest, Journal of Geophysical Research, 112, G02 020, https://doi.org/10.1029/2006JG000293, 2007.

Vitasse, Y., Lenz, A., Hoch, G., and Körner, C.: Earlier leaf-out rather than difference in freezing resistance puts juvenile trees at greater risk of damage than adult trees, Journal of Ecology, 102, 981–988, https://doi.org/10.1111/1365-2745.12251, 2014.

Vitra, A., Lenz, A., and Vitasse, Y.: Frost Hardening and Dehardening Potential in Temperate Trees from Winter to Budburst, New Phytologist, 216, 113–123, https://doi.org/10.1111/nph.14698, 2017.

Wickham, H., Averick, M., Bryan, J., Chang, W., McGowan, L. D., François, R., Grolemund, G., Hayes, A., Henry, L., Hester, J., Kuhn, M., Pedersen, T. L., Miller, E., Bache, S. M., Müller, K., Ooms, J., Robinson, D., Seidel, D. P., Spinu, V., Takahashi, K., Vaughan, D., Wilke, C., Woo, K., and Yutani, H.: Welcome to the tidyverse, Journal of Open Source Software, 4, 1686, https://doi.org/10.21105/joss.01686, 2019.

Wilmking, M., van der Maaten-Theunissen, M., van der Maaten, E., Scharnweber, T., Buras, A., Biermann, C., Gurskaya, M., Hallinger, M., Lange, J., Shetti, R., Smiljanic, M., and Trouillier, M.: Global Assessment of Relationships between Climate and Tree Growth, Global Change Biology, 26, 3212–3220, https://doi.org/10.1111/gcb.15057, 2020.

Xu, K., Wang, X., Liang, P., An, H., Sun, H., Han, W., and Li, Q.: Tree-Ring Widths Are Good Proxies of Annual Variation in Forest Productivity in Temperate Forests, Scientific Reports, 7, 1945, https://doi.org/10.1038/s41598-017-02022-6, 2017.

Yao, Y., Joetzjer, E., Ciais, P., Viovy, N., Cresto Aleina, F., Chave, J., Sack, L., Bartlett, M., Meir, P., Fisher, R., and Luyssaert, S.: Forest Fluxes and Mortality Response to Drought: Model Description (ORCHIDEE-CAN-NHA R7236) and Evaluation at the Caxiuanã Drought Experiment, Geoscientific Model Development, 15, 7809–7833, https://doi.org/10.5194/gmd-15-7809-2022, 2022.

Yousefpour, R., Augustynczik, A. L. D., Reyer, C. P. O., Lasch-Born, P., Suckow, F., and Hanewinkel, M.: Realizing Mitigation Efficiency of European Commercial Forests by Climate Smart Forestry, Scientific Reports, 8, 345, https://doi.org/10.1038/s41598-017-18778-w, 2018.

Zang, C., Hartl-Meier, C., Dittmar, C., Rothe, A., and Menzel, A.: Patterns of Drought Tolerance in Major European Temperate Forest Trees: Climatic Drivers and Levels of Variability, Global Change Biology, 20, 3767–3779, https://doi.org/10.1111/gcb.12637, 2014.

Zeileis, A. and Grothendieck, G.: Zoo: S3 Infrastructure for Regular and Irregular Time Series, Journal of Statistical Software, 14, 1–27, https://doi.org/10.18637/jss.v014.i06, 2005.

Zimmermann, J., Hauck, M., Dulamsuren, C., and Leuschner, C.: Climate Warming-Related Growth Decline Affects Fagus Sylvatica, But Not Other Broad-Leaved Tree Species in Central European Mixed Forests, Ecosystems, 18, 560–572, https://doi.org/10.1007/s10021-015-9849-x, 2015.

Zohner, C. M., Mo, L., Renner, S. S., Svenning, J.-C., Vitasse, Y., Benito, B. M., Ordonez, A., Baumgarten, F., Bastin, J.-F., Sebald, V., Reich, P. B., Liang, J., Nabuurs, G.-J., De-Miguel, S., Alberti, G., Antón-Fernández, C., Balazy, R., Brändli, U.-B., Chen, H. Y. H., Chisholm, C., Cienciala, E., Dayanandan, S., Fayle, T. M., Frizzera, L., Gianelle, D., Jagodzinski, A. M., Jaroszewicz, B., Jucker, T., Kepfer-Rojas, S., Khan, M. L., Kim, H. S., Korjus, H., Johannsen, V. K., Laarmann, D., Lang, M., Zawila-Niedzwiecki, T., Niklaus, P. A., Paquette, A., Pretzsch, H., Saikia, P., Schall, P., Šebeň, V., Svoboda, M., Tikhonova, E., Viana, H., Zhang, C., Zhao, X., and Crowther, T. W.: Late-Spring Frost Risk between 1959 and 2017 Decreased in North America but Increased in Europe and Asia, Proceedings of the National Academy of Sciences, p. 201920816, https://doi.org/10.1073/pnas.1920816117, 2020.